

Surface-normal 3×3 non-blocking wavelength-selective crossbar using polymer-based volume holograms

Charles Zhou and Ray T. Chen^{a)}

Microelectronics Research Center, University of Texas—Austin, Austin, Texas 78712

(Received 28 June 1996; accepted for publication 24 October 1996)

We present a 3×3 surface-normal wavelength-selective crossbar using polymer-based volume holograms. A prototype device is demonstrated using the center wavelength of 775 nm and $\Delta\lambda=10$ nm. Employment of $\frac{1}{4}$ -pitch graded-index rod lenses reduces the required nine wavelengths to three while maintaining the 3×3 interconnects. The diffraction efficiencies of 75%, 83%, and 75% are experimentally confirmed for wavelength 765, 775, and 785 nm, respectively. Surface-normal configuration eliminates the conventional edge-coupling scheme which is vulnerable in a harsh environment. A 3×3 crossbar is demonstrated with a two-way system insertion loss less than 3 dB and channel-to-channel cross talk less than 20 dB. © 1996 American Institute of Physics. [S0003-6951(96)04552-4]

Crossbar-based optical interconnects represent the most desirable network due to their fast switching speed and low latency in transmitting high speed signals. In this letter, we report the formation of a surface-normal nonblocking crossbar based on a unique wavelength switching scheme in which photopolymer-based volume holograms are employed in conjugation with graded index (GRIN) rod lenses. A prototype polymer-based volume hologram for multiple-wavelength 3×3 crossbar is experimentally demonstrated at 765, 775, and 785 nm. The unique beam routing property of a GRIN lens reduces nine wavelengths to three wavelengths while maintaining the required nine (3×3) individual interconnects. The elimination of edge-coupling significantly enhances the packaging reliability. Furthermore, such a configuration is compatible with the implementation of vertical cavity surface-emitting lasers where the characteristic of azimuthal symmetry may be maintained in the waveguide substrate.¹

The demonstrated device is shown in Fig. 1. The volume phase gratings recorded in the photopolymer films are slanted. The central wavelength of the input surface-normal beam, i.e., 775 nm, is designed to be diffracted with a maximum efficiency at the Bragg angle² which is 45° in our design. The wavelengths that deviate from the center wavelength are dispersed at different substrate bouncing angles with less diffraction efficiencies where discrete substrate modes are generated and zig-zagged within the substrate.³ The schematic of the microstructure of the designed volume holograms is shown in Fig. 2. The central wavelength bouncing angle θ_0 is set at 45°. For maximum diffraction efficiency at the central wavelength, the grating spacing Λ must satisfy³

$$\theta_0 = 2 \sin^{-1} \left(\frac{\lambda_0}{2n\Lambda} \right), \quad (1)$$

where λ_0 is the central wavelength, Λ is the grating spacing and n is the polymer refractive index.

Four GRIN rod lenses are employed for this demonstration. The three input GRIN lenses function as collimators for the incoming optical signals while the output GRIN rod lens functions as a focusing element on which a fiber array is integrated (Fig. 1). The GRIN lenses employed have a parabolic refractive index distribution profile of

$$n(y) = n(0) \left(1 - \frac{A^2}{2} y^2 \right), \quad (2)$$

where $n(0)$ is the refractive index of the GRIN lens axis and A is the GRIN lens property constant. The paraxial equation describing the ray position at the output GRIN lens surface from a zigzag substrate mode with a bouncing angle $\Delta\theta$ away from the Bragg condition is⁴

$$y(L) = y_0 \cos(AL) + \frac{\tan(\Delta\theta)}{A} \cdot \sin(AL), \quad (3)$$

where

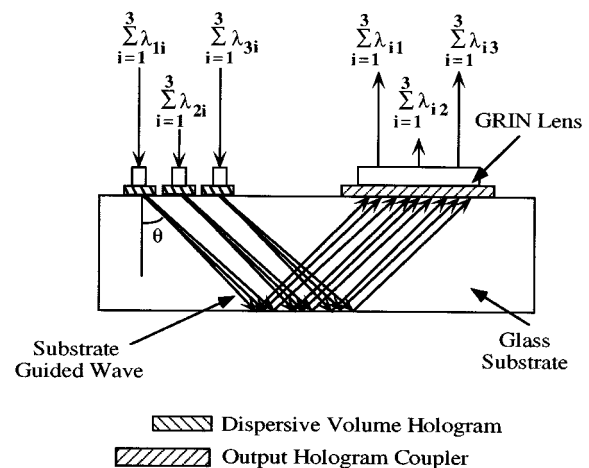


FIG. 1. Polymer-based volume hologram crossbar for a surface-normal 3×3 nonblocking wavelength selective crossbar. Note that the special characteristic of the GRIN lens reduces the nine wavelengths to three, i.e., $\sum_{i=1}^3 \lambda_{i1} = \lambda_1 = 765$ nm, $\sum_{i=1}^3 \lambda_{i2} = \lambda_2 = 775$ nm, and $\sum_{i=1}^3 \lambda_{i3} = \lambda_3 = 785$ nm.

^{a)}Electronic mail: raychen@uts.cc.utexas.edu

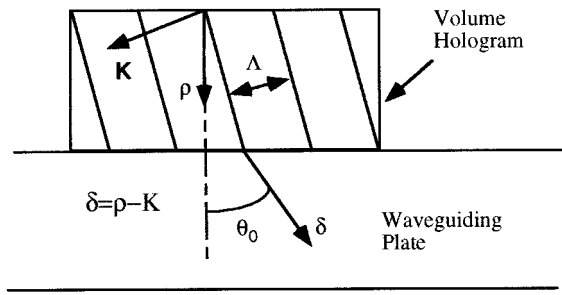


FIG. 2. Phase grating diagram showing phase-matching condition. \mathbf{K} , ρ , and δ represent the grating vector, the input wave vector and the output wave vector, respectively.

$$L = \frac{2\pi p}{A}. \quad (4)$$

In Eq. (4), p is the pitch size of the GRIN lens. Note for a quarter pitch lens, i.e., $p = 1/4$, only the second term of Eq. (3) exists. Consequently, incoming beams with the same wavelength and $\Delta\theta$ come out from the same spot at the output surface of the GRIN lens. In our experiment, the corresponding λ_{ij} and $\Delta\theta$ for each case of the 3×3 crossbar interconnects are summarized in Table I. Three GRIN lenses with 1 mm diameter each are used to collimate optical signals to the input holographic coupler (Fig. 1). An output GRIN lens is used to separate channels with different zigzag bouncing angles. At the surface of output GRIN lens, rays with the same initial bouncing angle converge to the same spot as predicted by Eq. (3). Therefore, employment of a GRIN lens reduces nine wavelengths to three wavelengths while keeping the required 3×3 interconnects. Combining our crossbar with the fast switching wavelength tunable VCSELs,⁵ a nonblocking 3×3 crossbar interconnect with a nanosecond (10^{-9}) switching speed can be realized. The bouncing angle differences are provided by the intrinsic dispersion of the input volume hologram. The use of GRIN lenses provides the capability of surface normal coupling through holograms and fibers. The vulnerable edge coupling scheme is eliminated. A reliable miniaturized package can thus be provided.

In the configuration shown in Fig. 1, three input fibers each with a collimating GRIN lens are attached surface-normally to the input volume hologram coupler. The three wavelengths transmitted through one single fiber are dispersed by volume hologram into three different bouncing angles. The bouncing angle deviation from the center wavelength is described by the coupled wave theory² which gives

TABLE I. Corresponding wavelengths and $\Delta\lambda$ s of the nine interconnects for 3×3 nonblocking crossbar.

Output\Input	1	2	3
1	$\Delta\theta=0.5^\circ$ $\lambda_{11}=765$ nm	$\Delta\theta=0.5^\circ$ $\lambda_{21}=765$ nm	$\Delta\theta=0.5^\circ$ $\lambda_{31}=765$ nm
2	$\Delta\theta=0^\circ$ $\lambda_{12}=775$ nm	$\Delta\theta=0^\circ$ $\lambda_{22}=775$ nm	$\Delta\theta=0^\circ$ $\lambda_{32}=775$ nm
3	$\Delta\theta=0.5^\circ$ $\lambda_{13}=785$ nm	$\Delta\theta=0.5^\circ$ $\lambda_{23}=785$ nm	$\Delta\theta=0.5^\circ$ $\lambda_{33}=785$ nm

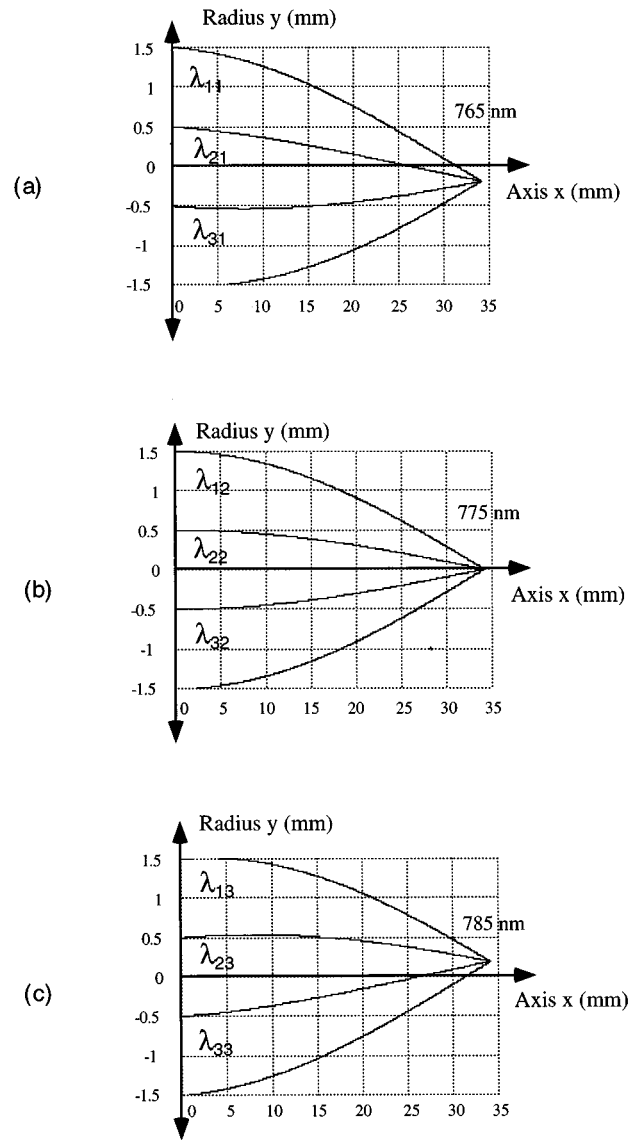


FIG. 3. Ray tracing of light with different incident angles from three input angularly dispersed light beams onto the quarter pitch output GRIN lens (a) $\sum_{i=1}^3 \lambda_{i1} = \lambda_1 = 765$ nm, (b) $\sum_{i=1}^3 \lambda_{i2} = \lambda_2 = 775$ nm, and (c) $\sum_{i=1}^3 \lambda_{i3} = \lambda_3 = 785$ nm.

$$\Delta\theta = \frac{2\Delta\lambda}{\lambda_0} \tan \frac{\theta_0}{2}, \quad (5)$$

where λ_0 is the center wavelength, $\Delta\lambda$ is the wavelength deviation from the center wavelength and θ_0 is the bouncing angle for the center wavelength corresponding to the perfect phase matching condition. As described by Eq. (3), a quarter pitch output GRIN lens separates light beams with different bouncing angles. $\Delta\theta$ is experimentally determined to be $\pm 0.5^\circ$ with $\lambda_0 = 775$ nm and $\theta_0 = 45^\circ$. These results are in good agreement with the theory. The signal beams with a same wavelength from three separate input fibers are thus routed to the same spot at the output surface of the quarter pitch GRIN lens (Fig. 3), where a fiber array is attached (three fibers in our case). Therefore by using only three wavelengths, a nonblocking 3×3 crossbar can be realized. The address of the sender in this case can be identified through the header encoded in the optical signal.⁶

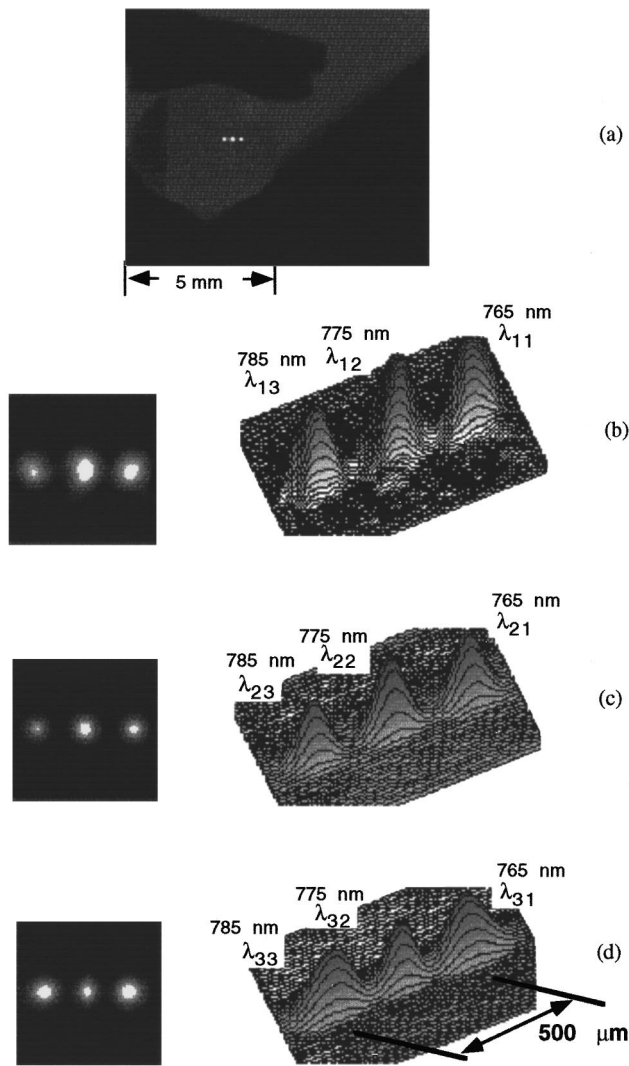


FIG. 4. (a) Image of GRIN lens output surface showing three-wavelength channel separation (b)–(d): two-dimensional and three-dimensional near field output mode profiles observed at the end of the output lens by activating (b), the first input channel, (c), the second input channel, and (d) the third input channel.

The experiment is conducted using a *p*-polarized Ti:sapphire tunable laser pumped by a continuous argon ion laser. DuPont polymer film HRF-600 having a thickness of 20 μm is employed and the hologram is recorded at 514 nm. The volume hologram is fabricated using a two beam interference method.⁷ The wavelength diffraction efficiencies of 75%, 83%, and 75% are experimentally obtained for 765, 775, and 785 nm, respectively.¹ A microscopic objective couples the light into a single mode fiber which has a GRIN rod lens attached at the output end. The input wavelength is monitored by an optical spectrum analyzer. The collimated light from the single-mode fiber is diffracted by the input holo-

TABLE II. The measured result of three-wavelength nonblocking crossbar.

Wavelength (nm)	Spot size (3 dB) (μm)	Channel separation (μm)
$\lambda_1=765$ nm	75 μm	250
$\lambda_2=775$ nm	75 μm	
$\lambda_3=785$ nm	75 μm	

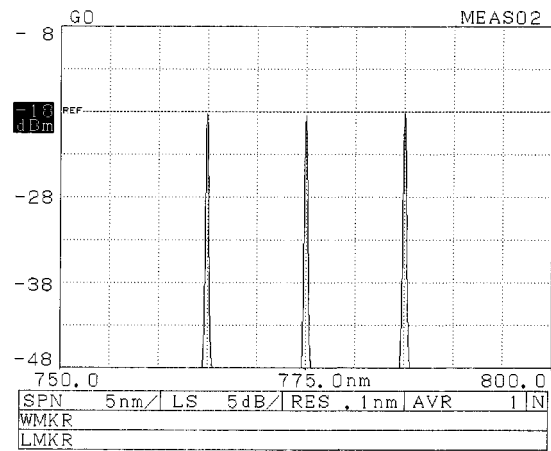


FIG. 5. Output spectrum of the 3 \times 3 crossbar at channels 765, 775, and 785 nm.

graphic coupler and zig-zagged inside the glass substrate. It is subsequently coupled out by the output hologram shown in Fig. 1. The output GRIN rod lens focuses the light onto different spots corresponding to different wavelength channels. A charge coupled device (CCD) camera and an eight bit frame grabber image processing system is employed to take the pictures. Spot size, channel separation and other parameters are experimentally confirmed in Fig. 4. In our experiment, the average channel separation is 250 μm and average spot size less than 75 μm . The average crosstalk is less than -20 dB. The result is summarized in Table II. The results shown in Fig. 4 represents incoming optical signals from one input fiber having three different wavelengths. The output spectrum corresponding to the output spots shown in Fig. 4 is further illustrated in Fig. 5. The output spectrum has the same bandwidth as that of the input (not shown). The measured two-way insertion loss is less than 3 dB. We have not observed any unwanted spectral shift due to scattering in all nine interconnects.

In summary, we present a surface-normal nonblocking crossbar based on the wavelength dispersion of a volume hologram. A 3 \times 3 crossbar containing nine interconnections has been successfully demonstrated with wavelengths of 765, 775, and 785 nm. The unique beam routing property of the GRIN lenses reduces the required nine wavelengths to three while maintaining the 3 \times 3 interconnects. Realizing the fact that the switching speed of semiconductor lasers can be as fast as 1 ns, we expect to demonstrate a feasible fully-integrated crossbar using the demonstrated concept.

This research is sponsored by AFOSR, BMDO, the ATP program of the state of Texas, and ARPA's Center for Optoelectronics Science and Technology.

¹Maggie M. Li and Ray T. Chen, Opt. Lett. **20**, 797 (1995).

²H. Kogelnik, Bell Syst. Tech. J. **48**, 2909 (1969).

³Maggie M. Li and Ray T. Chen, Appl. Phys. Lett. **66**, 262 (1995).

⁴W. M. Rosenblum, J. W. Blaker, and M. G. Block, Am. J. Optometry Physiological Optics **65**, 661.

⁵C. Chang, IEEE J. Quant. Electron. **27**, 1368 (1991).

⁶IEEE Standard for Scalable Coherent Interface (SCI), IEEE STD 1596 (1992).

⁷R. T. Chen, S. Tang, M. M. Li, D. Gerold, and S. Natarajan, Appl. Phys. Lett. **63**, 1883 (1993).